NANO LETTERS
Letter
Cite This: Nano Lett. XXXX, XXX, XXX−XXX
pubs.acs.org/NanoLett

Heavy Metal-Free Tannin from Bark for Sustainable Energy Storage

Alolika Mukhopadhyay,[†] Yucong Jiao,[†] Rui Katahira,[‡] Peter N. Ciesielski,[‡] Michael Himmel,[‡] and Hongli Zhu*

[†]Department of Mechanical and Industrial Engineering, Northeastern University, Boston, Massachusetts 02115, United States
[‡]National Renewable Energy Laboratory, Denver West Parkway, Golden, Colorado 80401, United States

Supporting Information

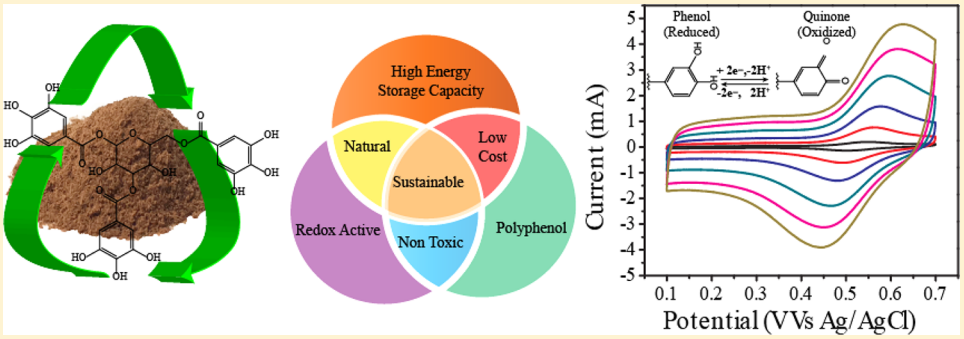

ABSTRACT: A novel renewable cathode made from earth abundant, low-cost materials can contribute to the intermittent storage needs of renewable energy-based society. In this work, we report for the first-time tannin from Nature as a cathode material. Our approach exploits the charge storage mechanism of the redox active quinone moiety. Tannins extracted from tree bark using environmental friendly aqueous solvents have the highest phenol content (5.56 mol g^{-1}) among all the natural phenolic biopolymers, 5000 times higher than lignin. Tannins coupled with a conductive polymer polypyrrole acquire high specific capacitance values of 370 F g^{-1} at 0.5 A g^{-1} as well as excellent rate performance of 196 F g^{-1} at 25 A g^{-1}. Additionally, we employed carbonized wood as an electrode substrate to produce a sustainable electrochemical device with dramatically improved performance compared to conventional devices. The high surface area provided by the well-aligned, cellular porosity of wood-derived substrate combined with the high mobility of ions and electrons in the carbonized cell walls and deposited tannin can achieve an areal capacitance of 4.6 F cm^{-2} at 1 mA cm^{-2}, which is 1.5 times higher than activated wood carbon.

KEYWORDS: *Tannins, electroactive phenol, bioinspired, cathode, carbonized wood, renewable, biopolymer*

The recent immense interest in optimal energy storage systems has been driven by a surging need for robust and affordable storage for intermittent renewable energy, exemplified by electric vehicles and consumer electronics.[1] Apart from the performance and safety related concerns, the biggest challenges for the advancement of future energy storage are the high cost of material synthesis and the shortage of metal-rich materials.[2] Currently, electrochemical energy storage primarily depends on extensive use of metal-based components, which are clearly not renewable materials. In contrast, the sustainable, low-cost, earth-abundant, and biodegradable materials with inherent faradic charge storage capabilities are excellent candidates to meet the massive societal energy storage demands of the future.[3,4] To meet these requirements, active redox polymers are appropriate, as they are environmentally friendly and recyclable as well as sustainable and metal free.[5] Among several suitable redox polymers,[6,7] those containing quinones have drawn considerable attention due to their excellent electrochemical performance, shown by very high energy storage capacity and high reversibility.[5,8,9] Naturally produced biopolymers that are rich in phenol and quinone moieties are widely available in plants and woods and can be harnessed for energy storage after low-cost purification. So far, redox-active lignin is the most studied biomass-derived polymer with intrinsically reversible electrochemical performance.[10] Although lignin has been studied extensively due to its abundance, their limited content of phenolic functional groups relative to their complex structure and high molecular weights has posed challenges for its use in high energy density energy storage systems.[5,11−13] Tannins can be grouped among the most abundant and versatile redox active biopolymers found in Nature and produced by natural plant biosynthesis. Tannins have molecular weights ranging from ∼500 to 20 000 Da.[14] On the basis of structural characteristics, tannins can be classified into two distinct categories, (1) hydrolyzable and (2) condensed forms. The low molecular weight (∼500 to 5000 Da) hydrolyzable tannins are highly water-soluble and can be further grouped into gallotannins and ellagitannins.[15] In the gallotannins, galloyl units are bound to polyol catechin (Figures

Received: October 4, 2017
Revised: November 6, 2017
Published: November 21, 2017

DOI: 10.1021/acs.nanolett.7b04242
Nano Lett. XXXX, XXX, XXX−XXX

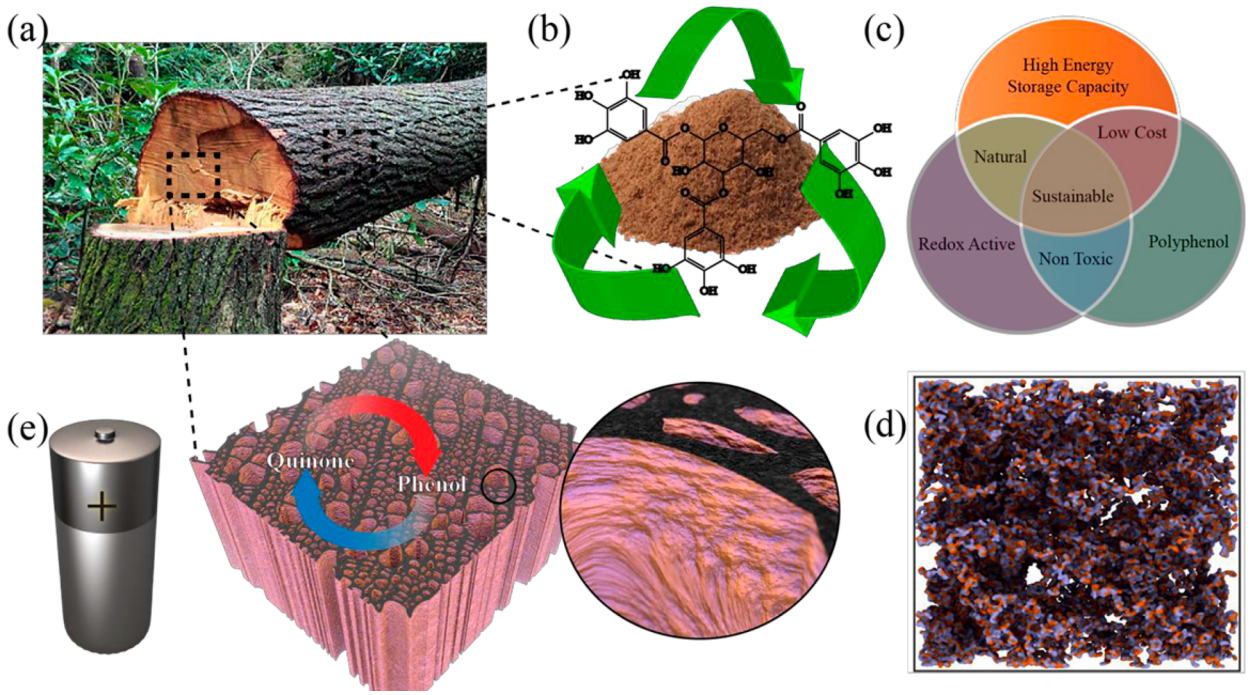

Figure 1. Schematic representation of the design and mechanism of the tannins/polypyrrole interpenetrating network as a renewable cathode. (a) Tannins are widely distributed in the bark of trees. (b) Tannin powder is prepared by vacuum drying after purification following the initial extraction from bark using an aqueous solvent. The molecular structure is representative of the stereochemistry of tannins. (c) Multivariant aspects of tannins for use as a sustainable cathode material. (d) Schematic representation of the interpenetrated network of tannins/polypyrrole. (e) The tannins/polypyrrole composite deposited on a carbonized wood as a freestanding cathode. The inset exhibits the growth of tannins inside the well-aligned channel walls along with the outer surface of the carbonized wood electrode.

S1 and S2), and in the ellagitannins at least two galloyl units are C−C coupled to each other (ellagitannins at least two Figure S3).[16] The condensed tannins have relatively higher molecular weights than the hydrolyzable tannins and are composed of flavon-3-ol oligomer groups as well as polymers linked by carbon−carbon bonds between flavonol subunits (Figures S4 and S5).[17] Tannins are widespread in the plant kingdom and typically found in the bark of the plants. The bark is predominantly acquired as a byproduct of the wood collection process, where the bark is approximately 12 to 16% tannins by weight.[18] In addition, the extraction of tannins from bark does not rely on toxic organic solvents; instead, one can use environmental friendly aqueous solvents, which offers a distinct advantage as it minimizes the environmental impacts of production and reduces the cost of material synthesis.[19] Tannin is extracted from the bark by immersing the dried bark in aqueous solvent and shaking either at room temperature for ∼8−10 h or by boiling for ∼10−15 min. The samples are filtered for purification, where only the residues are collected. Furthermore, the extracts are usually concentrated in a rotary evaporator and then dried in an oven at ∼50−60 °C until a solid powder is obtained.[20] By virtue of the extensive environmental and economic benefits, it is apparent that the valorization of tannins will add substantial value to the global economy. In addition to the arguments posed above, another motivation for using redox active biopolymers for sustainable energy storage is driven by the energy conversion process in plants, where Nature already uses redox active biopolymers. In the metabolism of plants and bacteria, electron and proton storage pathway are known; for example, quinones are used as soluble electron/proton transport agents. Nature exploits a four-electron photochemical oxidation process in photosynthesis where quinone acts as an electron acceptor to dissociate water into dioxygen and protons to transduce light into chemical energy.[21] Inspired by energy transfer in Nature, we employed quinone moieties as an energy storage and transport medium in renewable cathode material from the natural biopolymer, tannins. By exploiting its high phenol content, which can be converted to quinone, we have shown that tannins are promising energy storage materials.

Beyond the energy conversion process, Nature also creates a fascinating and sophisticated hierarchical cellular structure consisting of well-aligned, vertical channels in the growth direction of wood that transport water, nutrients, and ions throughout the plant. In addition, these well-aligned channels that form the microstructure of wood are also naturally beneficial for electrode design, as they provide percolated networks to facilitate electrolyte and ion transportation and effectively increase the mass loading by providing very high active surface area.[22,23] Therefore, to design an efficient, sustainable electrode, we further employed Nature's solution for ion and electrolyte transportation by reutilizing carbonized wood as a freestanding substrate with which to create a renewable cathode for sustainable energy storage. Use of carbonized wood will help to a highly scalable and low-cost electrode with enhanced performance and sustainability.

Herein, we report the discovery that tannins can serve as an earth-abundant energy storage electrode. To the best of our knowledge, the charge storage capacity of tannins has never been explored before. Our study revealed that tannins possess a discharge capacity of ∼370 F g^{-1} at 0.5 A g^{-1}, owing to their rapid and reversible conversion between the quinone and phenol moiety that is comparable to other known renewable energy storage materials.[12] Tannins have the highest phenol

DOI: 10.1021/acs.nanolett.7b04242
Nano Lett. XXXX, XXX, XXX−XXX

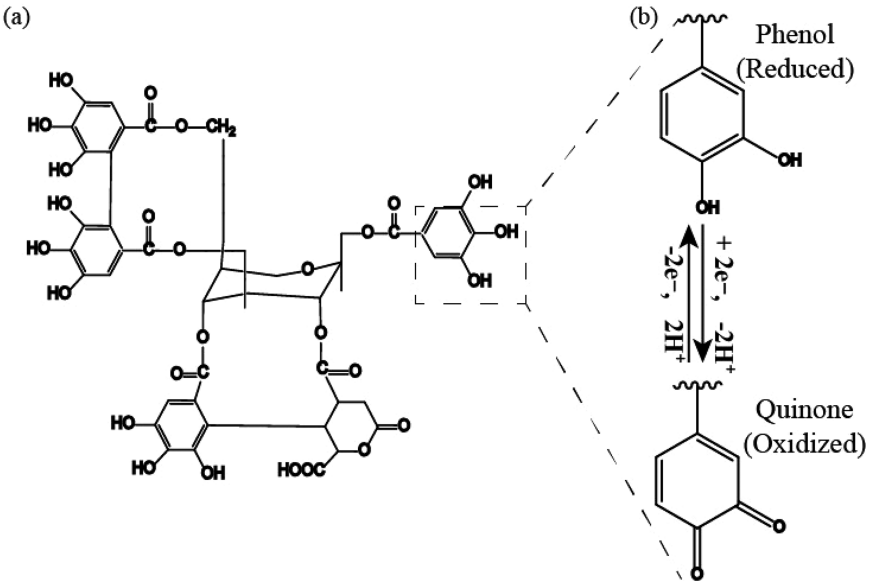

Figure 2. Charge storage mechanism of tannins through a rapid and reversible redox reaction. (a) The model structure is representative of ellagi tannins. (b) The magnified view shows the two electrons and two protons required for this rapid and reversible redox reaction between phenol and quinone.

content among all the natural phenolic biopolymers, orders greater than lignin.[14,12,24] This high phenol content trait of tannins potentially provides a much greater number of active functional groups for redox reaction, which in turn delivers a much higher capacitance and render tannins particularly attractive for energy storage applications. Furthermore, tannins were integrated within a conductive polypyrrole (Ppy) polymer (termed as Tn/Ppy) because of its insulating characteristic and high aqueous solubility. The conjugated polypyrrole polymer effectively prevents the dissolution of tannins into the aqueous solution and provides sufficient electronic conductivity to facilitate electron transport from its active quinone sites, which makes a major fraction of tannins accessible for electrochemistry. Therefore, tannins/polypyrrole composites were synthesized by oxidative electropolymerization on gold-coated silicon chips to investigate the fundamental electrochemistry of tannins and on sustainable carbonized wood in order to prepare a free-standing cathode entirely from biomass. Once produced, the tannins/polypyrrole composites on a gold-coated silicon chip showed a capacitance of 370 F g^{-1} at the 0.5 A g^{-1} current density and retained 196 F g^{-1} at a high current density of 25 A g^{-1}. In addition, tannins deposited on carbonized wood displayed an average areal capacitance of 4.6 F cm^{-2} at a current density of 0.5 mA cm^{-2} and retained capacitance of 3.95 F cm^{-2} at the current density of 3 mA cm^{-2}.

Rational Design of Tannins-Polypyrrole Cathode. Humans have been using wood as a source of energy for thousands of years by burning biomass. Today, people burn fossil fuels to release the energy that ancient plants captured from the sun. Biofuels encompass the solid, liquid, or gaseous fuels derived from biomass. All of the aforementioned energies are derived from the sun, captured by biomass via photosynthesis. However, the process of burning biomass has a low efficiency and comes with CO_2 emission. We propose an alternative application for the valuable biopolymers found in wood, wherein redox-active tannins from the bark of trees (depicted in Figure 1a) are used as electrode-active materials for clean and low-cost energy storage. The light brown colored fine powders (Figure 1b) of hydrolyzable ellagitannins extracted from bark of the chestnut tree were used for this study. As mentioned above, the redox active polyphenol tannins have many advantages for their use as a cathode material, because tannins not only have high charge storage capacity but are also sustainable, low-cost, and nontoxic because they are naturally occurring biopolymer (Figure 1c). Therefore, the renewable Tn/Ppy cathode can be prepared very easily by oxidative electropolymerization of pyrrole in aqueous tannins solution, where the perchloric acid ($HClO_4$) acts as the primary oxidant. Because of very high molecular miscibility of pyrrole and tannins, pyrrole entangles with tannin molecules during its polymerization and forms an interpenetrating network of polypyrrole and tannins Figure 1d.[10]

On the basis of our selection of carbonized wood as the substrate, it was apparent that the unique porous architecture of the electrode, as illustrated in Figure 1e, is of great importance for effective utilization of tannins as a sustainable cathode material. The inset of Figure 1e schematically elucidates the growth of tannins on the well-aligned vertical channel walls as well as on the outer surface of the carbonized wood piece. The porous configuration of the carbonized wood substrate provides sufficient channels for the in situ growth of the Tn/Ppy composites[23] along with excellent electronic conductivity, which assists ion transportation by creating a "percolation pathway." Along with the porosity, the large surface area offered by the hierarchical anisotropic structure of carbonized wood (CW) enables high mass loading and prevents clustering of the interpenetrating network of tannins and polypyrrole.

Natural tannins contain high phenol group content and thus the primary charge storage characteristic of tannins is the reversible conversion of phenol to quinone. Figure 2a illustrates a model structure of hydrolyzable ellagitannins.[16] It is worth noting that tannins have substantial heterogeneity in their structures depending on the source. For visualization purpose, a model structure is used to represent redox-active ellagitannins. The magnified view in Figure 2b explains the redox conversion mechanism between phenol and quinone. The electroactive

DOI: 10.1021/acs.nanolett.7b04242
Nano Lett. XXXX, XXX, XXX−XXX

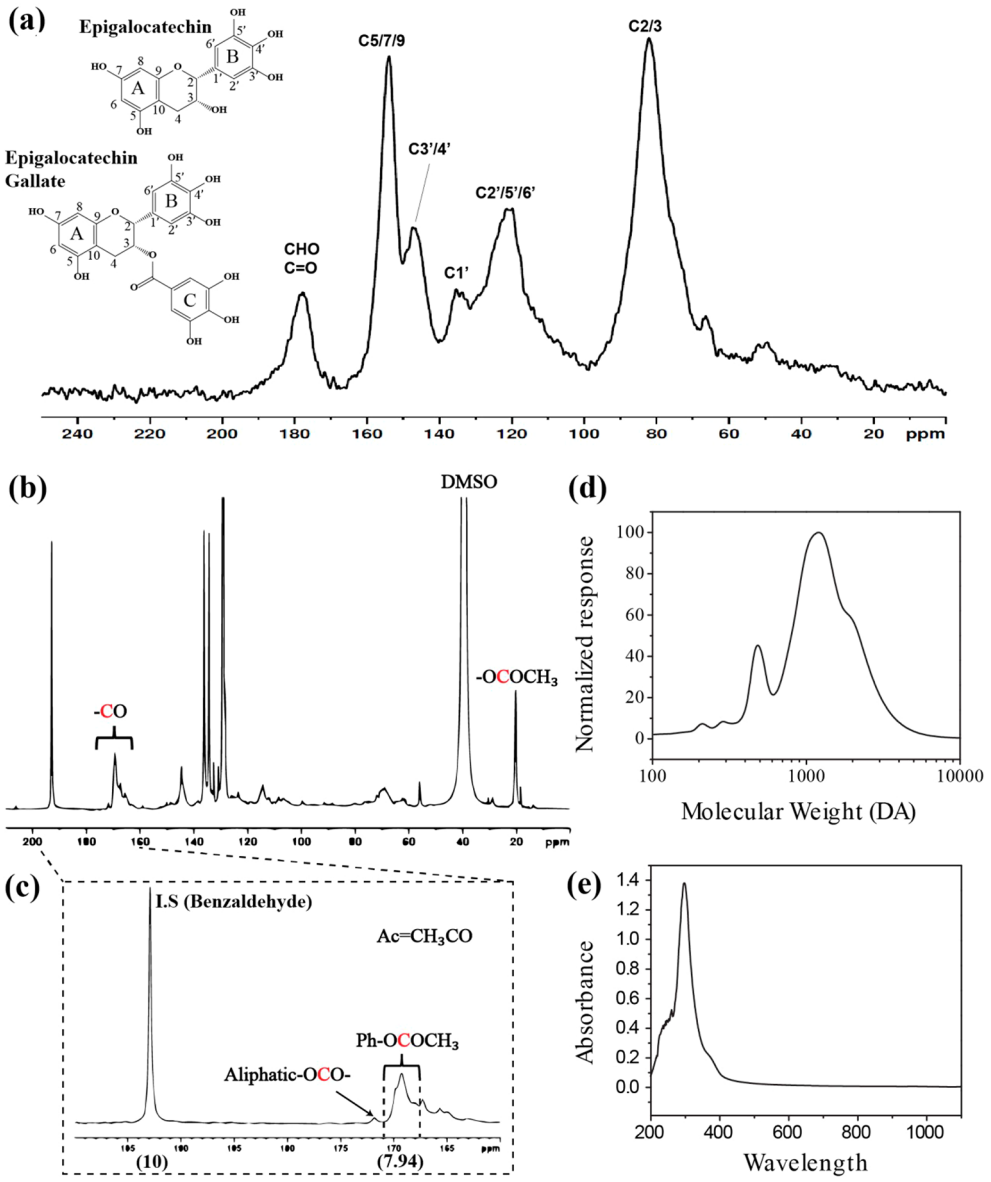

Figure 3. Structural and optical characteristics of hydrolyzable chestnut tannins. (a) Solid State ^{13}C CP/MAS NMR spectrum of hydrolyzable chestnut tannins displaying epigallocatechin monomer unit and carbonyl or aldehyde groups (b) Acylation-induced quantitative ^{13}C NMR spectra of hydrolyzable chestnut tannins exhibiting a strong phenolic-OAc peak at around 167.6−170.6 ppm. (c) Magnified view of the quantitative ^{13}C NMR spectra between 200 to 160 ppm showing phenolic and aliphatic acetyl peaks ($-OCOCH_3$). (d) Estimated molecular weight distribution of methylated chestnut tannins determined by gel permeation chromatography with polystyrene molecular weight calibration. (e) UV−vis spectra of hydrolyzable chestnut tannins within a wavelength range of 200−1000 nm showing a strong peak at 297 nm with two shoulders at around 260 and 360 nm.

phenolic hydroxyl radicals in tannins can be electrochemically oxidized and converted to quinones. The quinone moiety in tannins rapidly and reversibly accepts (or releases) two electrons and two protons during the charge (or discharge) process, yielding a high charge storage capacity.

Similarly, the charge storage mechanism of the Tn/Ppy composites is due to the perchlorate ion (ClO_4^-) insertion at the first step and release of two protons in the second step, as displayed in eqs 1 and 2, respectively.[10] Initially, due to the perchlorate ion insertion Ppy changes its oxidation state from 0 to 1 by leaving an electron. Subsequently, the phenol groups in tannins are modified by a redox reaction involving two electrons and two protons. The net reaction combining eq 1 and eq 2 is presented in eq 3

$$(\text{Tannin} - QH_2)\text{Ppy}^0 + HClO_4 \rightarrow (\text{Tannin} - QH_2)\text{Ppy}^+(ClO_4^-) + H^+ + e^- \quad (1)$$

$$(\text{Tannin} - QH_2)\text{Ppy}^+(ClO_4^-) \rightarrow (\text{Tannin} - Q)\text{Ppy}^+(ClO_4^-) + 2e^- + 2H^+ \quad (2)$$

$$(\text{Tannin} - QH_2)\text{Ppy}^0 + HClO_4 \rightarrow (\text{Tannin} - Q)\text{Ppy}^+(ClO_4^-) + 3e^- + 3H^+ \quad (3)$$

Structural Elucidation of Tannins. Much like lignins, tannins exhibit wide structural variations depending on their source. Even tannins found within a single plant species can exhibit substantial structural heterogeneity owing to pseudor-

DOI: 10.1021/acs.nanolett.7b04242
Nano Lett. XXXX, XXX, XXX−XXX

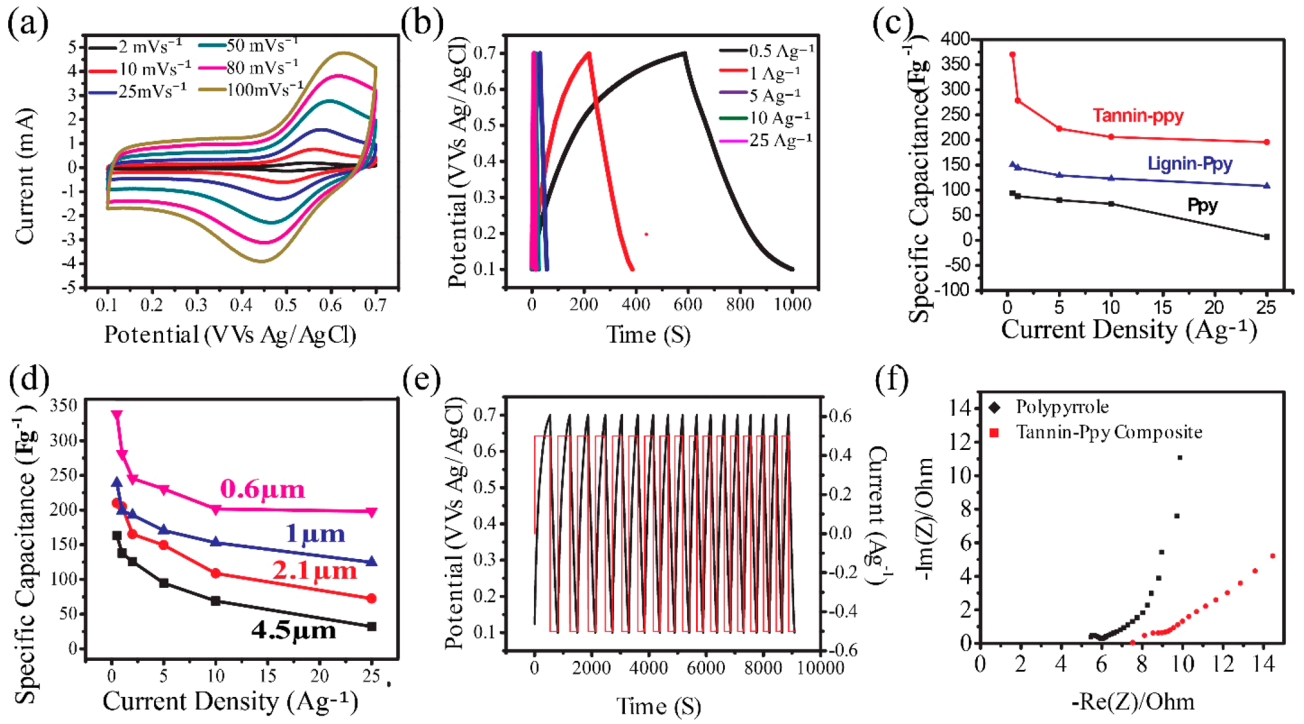

Figure 4. Fundamental electrochemical performance of the Tn/Ppy composites electrode on Au substrate. (a) Cyclic voltammetry profiles recorded between 0.1 to 0.7 V versus Ag/AgCl, scan rates 2−100 mVS^{-1} from inside to outside. (b) Rate performance at current densities ranging from 0.5 to 25 A g^{-1}. (c) Comparison of the gravimetric capacitance of Tn/Ppy, Lig/Ppy, and pure Ppy. (d) Galvanostatic discharge curves at 0.5 A g^{-1} current density. (e) Effect of thickness on the gravimetric capacitance of the Tn/Ppy composites electrode with different polymerization time (f) AC impedance spectroscopy of Tn/Ppy and pure Ppy shows three distinct regions; a semicircle followed by a Warburg region and a quasi-vertical line.

andom radical coupling processes during its biosynthesis. Consequently, the redox activities demonstrated by different kinds of tannins are not identical owing to the variations in their conformational details. Therefore, authentication of the conformation of the tannins used in this work was pursued. Because of the lack of its solubility in organic solvent, assessment of the overall structure was done by both solid state and solution state ^{13}C NMR. The signal assignment was performed according to the NMR data in literatures.[25−28] Carbon peaks on the ^{13}C NMR spectrum of the tannin sample shown in Figure 3a are consistent with the typical condensed/non-condensed tannins' pattern like procyanidin and epigallocatechin unit, which contains six hydroxyl groups. The peak at 150−158 ppm belongs to C5 and C7 attached to phenolic hydroxyl groups and C9 on the A-ring in epigallocatechin or procyanidins units. Peaks at 140−150 ppm belong to C3′ and C4′ on the B-ring. The signals at 132−140 ppm are for C1′. The peaks at 115−132 ppm belong to C2′, C5′, and C6′ on the B-ring. A small peak at 105 ppm is for the quaternary carbon at C10. There are geometric isomers at C2 and C3 position. C2 and C3 chemical shift in the 2,3-cis to 2,3-trans isomers could be slightly different. It was reported that C2 peak appears at 75.3 and 79 ppm for cis and trans form, respectively, and that C3 gives a resonance at 71.4 ppm in both cis and trans isomers.[27] Vazquez also reported that C3 peak in epigallocatechin usually appears at 72 ppm.[25] According to these NMR data, a large peak at 70−90 ppm could correspond to C3 in epigallocatechin unit. A small peak at 66 ppm is due to C3 of the terminal unit. A large carbonyl peak appears at 170−185 ppm, indicating that a large portion of epigallocatechin gallate unit is contained in the tannin sample.

Furthermore, acetylated tannins were analyzed by solution state ^{13}C NMR. ^{13}C NMR was also acquired to evaluate the phenolic hydroxyl groups of this tannin fraction quantitatively. Acetylation converted the phenolic-OH to phenolic-OAc ($-OCOCH_3$). The amount of free hydroxyl moiety was estimated using integration of carbonyl carbon in the acetyl group in the region of 167.6 to 170.6 ppm along with the intensity of the resonance (Figure 3b). Integrating the phenolic-OAc peak observed in Figure 3c and benzaldehyde used as an internal standard the phenolic hydroxyl content of the specimen was calculated to be 5.56 $molg^{-1}$. In contrast, according to the NMR data, the ultrafiltered lignosulfonate contains only 1.05 mmol g^{-1} phenolic-OH, which regulates the charge storage capacity of lignosulfonate (Figure S6). It was evident from the results that compared to lignin, the phenol content of tannins is ∼5000 times higher, which eventually leads to a higher specific capacitance of tannins compared to lignin. To further characterize the molecular weight distribution of this tannin preparation, gel permeation chromatography was carried out on a methylated tannin fraction with tetrahydrofuran as the mobile phase solvent. This specific tannin preparation showed a peak molecular weight (M_p) estimated as 1400 Da as well as several smaller, pauci-disperse components (see Figure 3d). Although lignin and tannins are structurally and biosynthetically related natural polyphenols, the average molecular weights of lignosulfonates are ∼5000−50 000 Da, which is substantially higher than the tannins.[10] Moreover, the low molecular weight along with the high phenol content increases the specific gravimetric capacitance of tannins compared to lignin. Therefore, tannins possess higher energy and power density on a mass basis than lignin.

DOI: 10.1021/acs.nanolett.7b04242
Nano Lett. XXXX, XXX, XXX−XXX

To seek further evidence about the presence of phenol rich hydrolyzable tannins, UV−vis spectroscopy was performed. UV−vis spectroscopy provides another effective means to identify hydrolyzable tannins distinctly.[29] We found that UV−vis spectra exhibited a strong absorption peak at 297 nm with a shoulder around 260 and 360 nm (Figure 3e). The peak at 297 nm is attributable to the epigallocatechin moiety due to the transition of an oxygen lone pair from nonbinding n-orbital of the C═O chromophore to π^* orbital in the UV−vis region. Thus, the strong peak at 297 nm with two sharp shoulders observed at 260 and 360 nm further verifies the existence of phenol rich hydrolyzable ellagitannins in the chestnut extract.[29] It was also obvious that tannins have distinct optical properties owing to their planar and semirigid backbone and π-conjugation.

Electrochemical Performance of Tannins. The electrochemical performance of Tn/Ppy composites on gold-coated silicon chips were evaluated at three electrode-setups using 0.1 M aqueous $HClO_4$ as the electrolyte. To better investigate the energy storage mechanism of tannins, cyclic voltammetry (CV) was conducted within a voltage window of 0.1 to 0.7 V versus Ag/AgCl. CV curves, as illustrated in Figure 4a, for Tn/Ppy electrodes obtained at varying scan rate from 2 to 100 mV s^{-1} reveal a very well-defined and sharp anodic peak at ∼0.54 V and a cathodic peak at ∼0.50 V versus Ag/AgCl corresponding to the reversible oxidation and reduction of the phenol groups[5,10,12] of tannins. The cathodic and anodic peak separation of 40 mV was close to the theoretically expected value of 59 mV/n for a Nernstian process (eq S1), where n is 2 and the theoretically expected value is 29.5 mV in this case because two electrons are involved in the redox reaction. This phenomenon represents highly reversible and rapid energy storage with small overpotential. Moreover, the dependence on the redox peak currents on scan rate[10,12] is indicative of an ion-adsorption dependent redox processes. To distinguish the redox activity of pure tannin from Tn/Ppy composite, cyclic voltammetry of a thin layer of pure tannin deposited on carbon paper was determined (as shown in Figure S9). The CV curves obtained at varying scan rate from 2 to 100 mVs^{-1} reveal a pair of very well-defined and sharp anodic peak at ∼0.57 V and a cathodic peak at ∼0.50 V versus Ag/AgCl corresponding to the reversible oxidation and reduction of the phenol groups. Therefore, it can be concluded that the oxidation and reduction peaks at 0.54 and 0.5 V for Tn/Ppy composite correspond to the redox of tannin only. To verify the redox activity of tannin in other electrolytes than 0.1 M $HClO_4$, the cyclic voltammetry of pure tannin deposited in carbon paper was also tested in 0.5 M H_2SO_4 and 1 M HCl. The CV curves obtained using 0.5 M H_2SO_4 display a pair of anodic peak at ∼0.57 V and a cathodic peak at ∼0.55 V versus Ag/AgCl corresponding to the reversible oxidation and reduction of the phenol groups (as shown in Figure S10). However, the CV curves obtained using 1 M HCl display a sharp cathodic peak corresponding to the reduction of phenol groups but the anodic peaks are not very well-defined. Therefore, it is also possible to use 0.5 M H_2SO_4 as a replacement of 0.1 M $HClO_4$, however, the redox activity of tannin is better in 0.1 M $HClO_4$ compared to any other electrolytes. To gain further insight into the electrochemical performance of the Tn/Ppy composites, galvanostatic charge−discharge in the potential window of 0.1 to 0.7 V versus Ag/AgCl was conducted, as shown in Figure 4b. The specific capacitance was derived from the same experiment using the slope of the linear part of the charge−discharge curves. To distinguish the capacity contribution of tannins and polypyrrole in the Tn/Ppy composites, pure Ppy deposited on the gold-coated silicon chip was used as a control sample and tested in the three electrode system (Experimental Section). Furthermore, to better assess the performance of Tn/Ppy, capacitance values were also compared to the lignosulfonate/Ppy (Lig-Ppy) composites under the same conditions. Figure 4c explicitly shows the attained specific capacitance values of active material Tn/Ppy, control sample pure Ppy, as well as the comparable sample Lig-Ppy. The specific capacitance values of tannins are approximately 370, 278, 222, 205, and 196 F g^{-1} at current densities of 0.5, 1, 5, 10, and 25 A g^{-1}, respectively. Conversely, the specific capacitance of pure Ppy are 94, 88, 80, 72, and 7 F g^{-1} and the Lig/Ppy are 151, 145, 129, 123, and 108 F g^{-1} at similar current densities of 0.5, 1, 5, 10, and 25 A g^{-1}, respectively, which are considerably less than the Tn/Ppy. Therefore, it was apparent that the high capacitance for Tn/Ppy resulted from the enormous content of phenol groups in tannins, which is consistent with results from the CV analysis. Also, the capacitance value obtained for pure Ppy is only 25% of the capacitance obtained for Tn/Ppy at a similar current density, which leads us to the conclusion that the capacity contribution of tannins is remarkably higher than Ppy in the Tn/Ppy electrode. In addition, more than 50% capacity retention of Tn/Ppy at a high current density of 25 A g^{-1} indicates an excellent rate capability that can be attributed to the superior ion and electron transfer kinetics as a result of the high electronic conductivity of Ppy. Therefore, these results indicate that the principal role of Ppy is to provide sufficient electronic conductivity to make the active phenol sites of tannin accessible for faradic reaction. More importantly, the specific capacitance values acquired for Tn/Ppy are more than two times higher than Lig/Ppy and surpasses our previously reported graphene-modified lignosulfonate electrode (211 F g^{-1} at 1 Ag^{-1})[12] at similar current densities. The observed high specific capacitance of Tn/ppy compared to Lig/Ppy corresponds to the order of magnitude higher phenol content and low molecular weight of tannins compared to lignin.

To study the dependence of charge storage capacity on the layer thickness of Tn/Ppy, the capacitance of the Tn/Ppy with varying layer thickness was evaluated. The mass and thickness of Tn/Ppy layers correlate almost linearly with polymerization time with an r^2 value of ∼0.982 and ∼0.81, respectively (Figure S7a,b). Furthermore, the specific capacitance values of Tn/Ppy of varying layer thickness are plotted in Figure 4d. It shows the capacitance values of Tn/Ppy range from 338 F g^{-1} (0.5 A g^{-1}) to 198 F g^{-1} (25 A g^{-1}), 239 F g^{-1} (0.5 A g^{-1}) to 125 F g^{-1} (25Ag^{-1}), 210 F g^{-1} (0.5 A g^{-1}) to 73 F g^{-1} (25 A g^{-1}), and 163 F g^{-1} (0.5 A g^{-1}) to 32 F g^{-1} (25 A g^{-1}) for 0.6, 1, 2.1, and 4.5 μm thick layers, respectively. It was evident from the achieved capacitance values that the thin Tn/Ppy films ensure very high capacitance with an excellent rate capability, whereas the thick and high mass loaded (Figure S7a) electrodes with thicknesses above 2 μm experience an eventual decrease in capacitance. This happens simultaneously, because of the reduction in accessibility of electrochemically active sites to ions with increasing thickness due to the extended diffusion path and the negligible electron storage capacity of the uppermost film that reduces the charge storage capability of the active material (tannins). Although the specific capacitance values gradually decrease with the increase in layer thickness, the capacitance values obtained for high mass loaded electrodes

DOI: 10.1021/acs.nanolett.7b04242
Nano Lett. XXXX, XXX, XXX−XXX

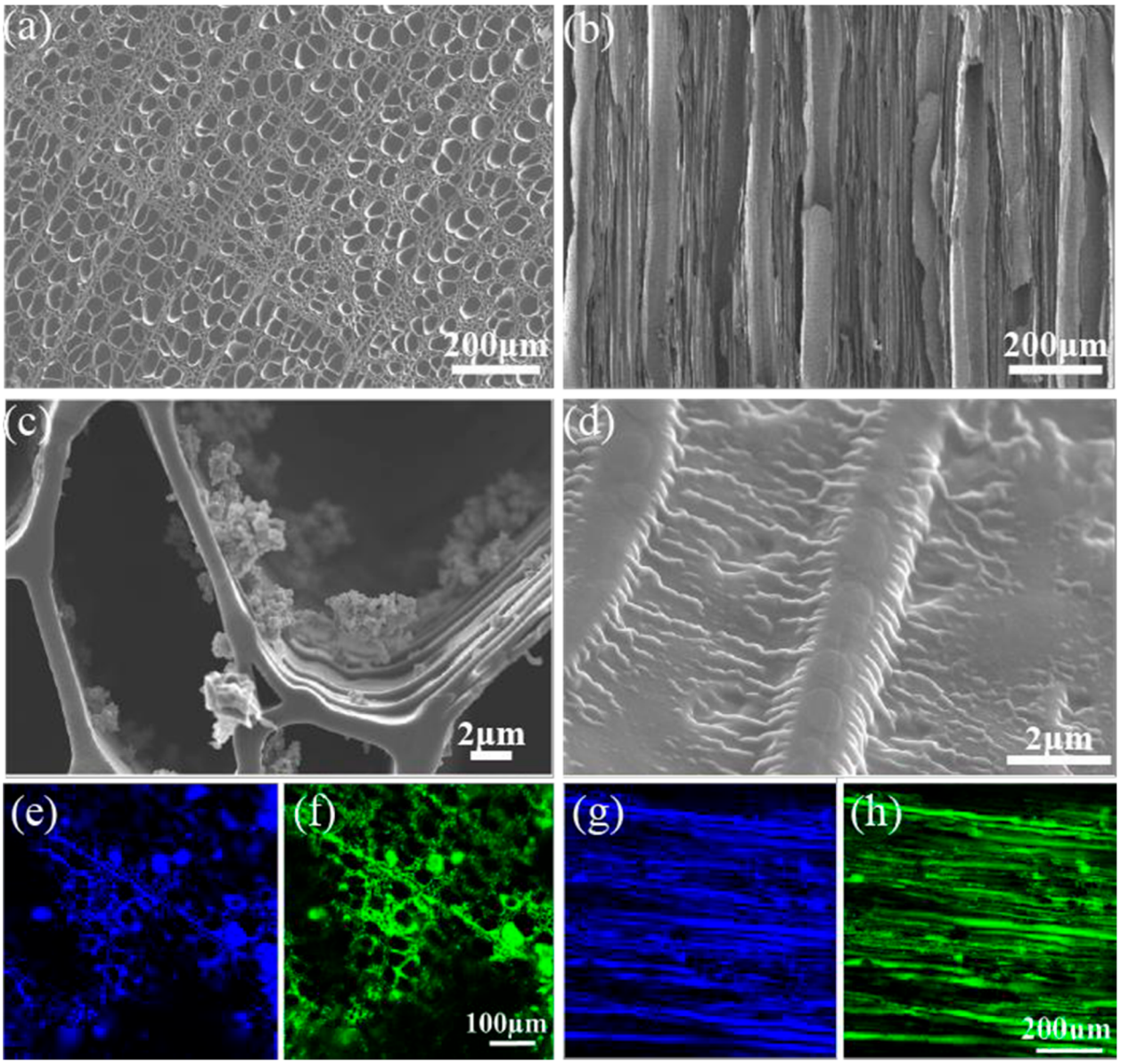

Figure 5. Scanning electron microscopy images of carbonized wood substrate and Tn/Ppy loaded renewable cathode. (a) Top-view image of the transverse cross-sectional cut of a carbonized wood substrate displaying porous architecture. (b) Top-view image of the longitudinal cross-section cut of a carbonized wood substrate showing well aligned vertical channels. (c) High-magnification top view image of the transverse cross sectional cut illustrating Tn/Ppy interpenetrating network grown on channel walls. (d) High-magnification high-angle image of the longitudinal section cut demonstrating an equally spaced island of Tn/Ppy composites on channel wall. Confocal images of tannin deposited on carbonized wood substrate showing a uniform distribution of tannin. The transverse cross section at 10× magnifications with (e) an excitation wavelength 405 nm and (f) an excitation wavelength 488 nm. The longitudinal cross section at 4× magnification with (g) an excitation wavelength 408 nm and (h) an excitation wavelength 488 nm.

are still exceptionally high and comparable to some of the current high mass loaded thick electrodes.[30,31]

To evaluate the performance stability of the composite electrode, the galvanostatic charge−discharge within a voltage window of 0.1 to 0.7 V versus Ag/AgCl was carried out at 0.5 A g^{-1} current density. The charge−discharge profiles for a few cycles with prolonging charge−discharge time of approximately 30 min for 0.6 mg cm^{-2} mass loaded electrode are shown in Figure 4e. A minimal potential hysteresis observed between the charging and discharging steps suggests rapid energy storage, which is in good accordance with CV curves. To further elucidate the electrochemistry of hydrolyzable tannins, the typical electrical impedance spectrum is presented as a Nyquist plot (see Figure 4f), which corresponds to the CV profiles. For both the Tn/Ppy and pure Ppy electrodes, EIS curves displayed three distinct regions, a semicircle followed by a Warburg region and a quasi-vertical line. The equivalent series resistance R_s (the first intercept with the real impedance axis) and the charge transfer resistance R_{ct} (the diameter of the semicircle at high frequency) are approximately 7 and 3 Ω for Tn/Ppy and 5 and 1 Ω for Ppy, respectively. These results explicitly indicated that a rapid charge transfer with very little internal resistance and fast-electrolytic ion diffusion kinetics is achieved as a consequence of the networks produced by the tannins and Ppy composites. The very high miscibility of tannins and Ppy presumably contribute to this outcome.

DOI: 10.1021/acs.nanolett.7b04242
Nano Lett. XXXX, XXX, XXX−XXX

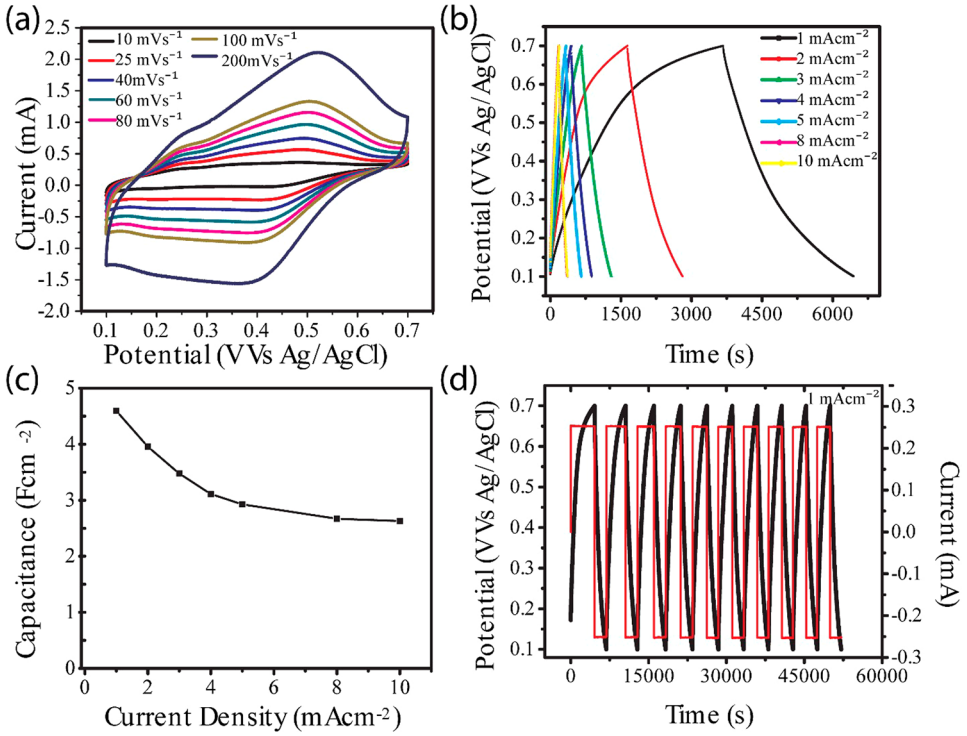

Figure 6. Electrochemical performance of Tn/Ppy composites electrode on carbonized wood substrate. (a) Cyclic voltammetry profiles recorded between 0.1 to 0.7 V versus Ag/AgCl, scan rates 10−200 mV s^{-1} from inside to outside. (b) Rate performance at current densities ranging from 0.5 to 25 A g^{-1}. (c) Comparison of the gravimetric capacitance of Tn/Ppy, Lig/Ppy, and pure Ppy. (d) Galvanostatic discharge curves at 1 mA cm^{-2} current density.

In summary, the performance of Tn/Ppy is comparable to that of the state-of-the-art earth abundant natural energy storage materials.[1,5,10−13,32] The excellent electrochemical performance of Tn/Ppy is likely due to the extremely high phenolic hydroxyl content of tannins, which can be reversibly converted to quinone through electrochemical oxidation, thereby storing energy. The high redox reversibility of tannins corresponds to the stable conformation of these compounds in an acidic environment. The key aspects of achieving high energy density are the low molecular weight and high mass loading of the active material (tannins). Although the selected tannins have significantly low molecular weight (M_p = ∼1400), there is a gradual reduction in achieved specific capacitances depending upon the thickness and mass loading of Tn/Ppy due to the restricted ion diffusion in the thickness direction, which eventually mitigates the energy density of the active material.

Practical Design and Characterization of Tannins Integrated with Carbonized Wood. Moreover, it is also worth noting that instead of having a stable conformation with an excellent specific capacitance, the cycling stability of tannins was not satisfactory. It was anticipated that the observed sharp decay in capacitance was predominantly due to the extremely high aqueous solubility of tannins, which led to the loss of effective capacitive material. Even though the complex physical network of Tn/Ppy aided in preserving the active material to a certain extent, loss of active material during cycling is still an area for future development toward the optimal use of tannins as cathode materials. Hence, the electrochemical performance of tannins can be further improved by further optimizing the synthesis process of the Tn/Ppy composites and tuning the configuration of the electrode. Therefore, to realize the full potential of this system we chose to use a porous electrode structure with open channels, which will provide an extremely high surface area; as well as accessible internal pathways to accelerate ion and electron transportation. We believe that our design of this novel electrode, containing conductive carbonized wood substrate, will meet our design criteria by providing well-aligned channels and increased mass loading per area without affecting the capacitance of Tn/Ppy. Constant current oxidative electropolymerization of pyrrole monomers in aqueous tannins solution in a three-electrode setup with the CW as a working electrode and 0.1 M perchloric acid as an oxidant was used to prepare the Tn/Ppy electrode. To depict the morphology and distribution of tannins inside the porous architecture of the freestanding electrode, scanning electron microscopy (SEM) images were obtained. The transverse cross-sectional cut of the CW (Figure 5a) exhibits two distinct, identically sized channels.The larger pores result from vessel cells in the original wood and exhibit diameters of ∼50 μm and the smaller, more abundant pores result from fiber cells and range from ∼10 to 15 μm in diameter. The longitudinal section cut (Figure 5b) shows deep channels and existence of numerous mesopores on the channel walls, which result from pits in the wood cell walls that served to connect adjacent cells. The nucleation and in situ three-dimensional growth of the complex physical network of Tn/Ppy on the channel walls were evidenced by the high-magnification SEM images of transverse and longitudinal cross sections (Figure 5c,d, respectively). Consistent with these results, the growth of the Tn/Ppy polymers was enabled inside the channel walls due to the small free-energy barrier for heterogeneous nucleation of Tn/Ppy. Carbonized wood is a form of carbon,[33] and according to the previously published literature it is well established that the adsorption of polymers and biomaterials are due to the van der

DOI: 10.1021/acs.nanolett.7b04242
Nano Lett. XXXX, XXX, XXX−XXX

Waals forces on the surface of the carbon materials.[32,34] Therefore, it was assumed to have noncovalent bonding between the Tn/Ppy composite and the carbonized wood substrate. It is not possible to positively identify the presence of deposited tannins in the electrode from SEM images because of the lack of contrast between tannins and Ppy material; however, the morphology difference between the materials seen in Figure 5c clearly shows the presence of a globular material adhered to the pore walls. Therefore, to directly visualize the distribution of tannins in the electrode, we performed scanning laser confocal microscopy. Tannins show a strong emission upon photoexcitation at a wavelength slightly higher than the absorption maxima, 405 and 488 nm, which is presumed to be a distinctive characteristic of tannins. Negligible background fluorescence and increasing fluorescence intensity with increasing tannins' concentration further endorsed the fluorescence property of tannins. The transverse cross-sectional cut of the electrode excited with 405 and 488 nm lasers showed similar emission intensity, yet the middle lamella between two adjacent walls was observed to have the strongest emission intensity. This result may be due to higher tannins deposition in both cases (Figure 5e,f). In contrast, longitudinal cross sections cut excited with 405 and 488 nm laser exhibited a uniform growth inside the CW channels due to its unique hierarchical porous structure (Figure 5g,h). Thus, the SEM and confocal images together verify the uniform in situ growth of Tn/Ppy on CW substrate.

Electrochemical Performance Evaluation of the Tn/Ppy Deposited CW Electrode. To better investigate the electrochemical performance of the Tn/Ppy deposited CW electrode, a typical cyclic voltammetry of the Tn/Ppy CW electrode was carried out within a potential range of 0.1−0.7 V versus Ag/AgCl reference electrode. Figure 6a shows cyclic voltammetry profiles with the appearance of a primary pair of current peaks at ∼0.50 and ∼0.45 V separated by ∼38 mV and a secondary pair of small peaks nearly at ∼0.24 and ∼0.19 V separated by ∼50 mV, associated with the reduction and oxidation of the quinone groups on the tannins. These results clearly demonstrate that the overpotential of the primary peaks for CW substrate is approximately 40 to 50 mV less compared to the Au substrate, where the reduction and oxidation peaks occur at ∼0.54 and ∼0.50 V, respectively. This low overpotential is likely attributed to the fast ion transportation along the well-aligned long channels with mesoporous structure as well as the fast electron transfer from the reaction sites resulting from the extremely high conductivity of the carbonized wood.[22] In addition, appearance of the second set of redox peaks, related to the oxidation and reduction of phenol groups in tannins, can be ascribed to the availability of the maximum number of active phenol groups in tannins for the intended redox reactions because of the uniform growth of Tn/Ppy inside the channel walls in a manner that prevents cluster formation as well as assists in the electrolyte diffusion to the Tn/Ppy network inside the channels. CVs attained at different scan rates also show the redox peak current dependency on scan rates, which are very similar to the Au substrate.

The charge−discharge profiles of Tn/Ppy CW electrodes at various current densities ranging from 0.5 to 10 mA cm^{-2} are presented in Figure 6b. From the discharge patterns, it is apparent that the charge−discharge time is very long, corresponding to the highly active functional groups (quinone) found in tannins, which receive electrons during discharging and release electrons during the charging process. Accordingly, the areal capacitance values, plotted in Figure 6c, are calculated from the charge−discharge profiles using the slope of the linear part. The average areal capacitance obtained for Tn/Ppy on CW are approximately 4.6, 4, 3.5, 3.1, 2.9, 2.7, and 2.6 F cm^{-2} at the current density of 1, 2, 3, 4, 5, 8, and 10 mA cm^{-2}, respectively. In contrast, areal capacitance of carbonized wood and carbonized wood loaded Ppy was also determined, which is much lower than the capacitance of Tn/Ppy on CW as shown in Figure S11 in the Supporting Information. At a very high current density of 10 mA cm^{-2}, the Tn/Ppy on CW obtains a capacity of 1 mA cm^{-2}. This high areal capacitance combined with the outstanding rate capability of Tn/Ppy deposited CW electrode is attributable to the hierarchical porous architecture of the conductive wood carbon substrate. This unique substrate contains high surface area in the form of a natural porous network and facilitates high mass uptake with uniform distribution of the Tn/Ppy. Moreover, the areal capacitance obtained for Tn/Ppy on CW electrode at 3 mA cm^{-2} is superior to previously reported areal capacitance of activated wood carbon (2.93 F cm^{-2}) at similar current density.[22] The Tn/Ppy CW electrode was also charged−discharged continuously at 1 mA cm^{-2} for an extended period of time without having much decay in its capacitance (Figure 6d), which confirms the reversibility of the redox reaction. Furthermore, this stability of the electrode is partly because of the carbonized wood substrate, which maintains its structural integrity for a long time in the acidic environment even at very significant high current density.

In summary, the outstanding performance of the Tn/Ppy on the CW electrode is likely due to the synergetic effect of the redox chemistry of tannins and the structural attributes of carbonized wood. Integrating the carbonized wood ultrastructure with the excellent redox properties of tannins further enhances the fundamental electrometrical performance of this natural material. The benefits of using CW as the substrate includes (1) in situ carbonization which provides high electronic conductivity while retaining its structural integrity, (2) low-tortuosity transverse channels in wood that assist in the ion transport through a percolation type pathway, and (3) high porosity that offers extremely large surface area, which enables high mass loading and prevents clustering of the Tn/Ppy.[35] However, irrespective of having all these benefits the coulombic efficiency of Tn/Ppy composite is not satisfactory at this stage and further development is needed to address this issue.

Conclusion. Through inspiration from Nature, we subjected the biopolymer, tannins, to rapid and reversible redox of its quinone and phenol groups. Low molecular weight tannins exhibit sufficiently high phenol content and capacitance to be exploited as a sustainable, low-cost cathode material for future green energy storage solutions. The redox active tannins can be extracted using safe and nontoxic aqueous solvents. Synthesis of tannin-based electrode to enable its electrochemical performance was carried out by mixing tannins and pyrrole monomer, followed by electropolymerization of the tannins and polypyrrole mixture on a gold current collector. Its specific capacitance was shown to be 370 F g^{-1} at 0.5 A g^{-1} with an excellent rate performance, whereas its capacity retention at a high current density (25 A g^{-1}) exceeded 195 F g^{-1}. To further enhance the performance of this system, we paired a carbonized wood electrode with the tannin and polypyrrole network to demonstrate a high-performance tannins electrode for practical application. This electrode achieved an areal capacitance value of 4.6 F cm^{-2} at 0.5 mA cm^{-2} with capacity retention of 2.6 F

DOI: 10.1021/acs.nanolett.7b04242
Nano Lett. XXXX, XXX, XXX−XXX

cm^{-2} at the higher current density of 10 mA cm^{-2}. The introduction of tannins as the redox active species opens up new directions for research and offers outstanding opportunities for the development of sustainable energy storage systems.

Experimental Section. *Materials.* Hydrolyzable chestnut tannins were supplied by Granit Corp. Lausanne, Switzerland. Reagent grade materials such as pyrrole, methanol, pyridine, acetic anhydride, tetrahydrofuran, tetramethylsilane, and chromium(III) acetylacetonate were obtained from Sigma-Aldrich and perchloric acid, toluene, and DMSO were obtained from Fisher. All chemicals were used as received and deionized water was used to prepare all solutions.

Synthesis of Tn/Ppy Composites. To prepare the Au substrate for electropolymerization, a Cr/Au (2 nm/120 nm) layer was sputtered on SiO_2 /Si (470 nm/380 μm) wafer and then diced into 12 mm × 12 mm chips. Correspondingly, for the preparation of carbonized wood substrate, a natural basswood block (purchased from Walnut Hollow Company, Dodgeville) was cut into desired thickness along the longitudinal direction and then pretreated at 250 °C for 4 h, followed by carbonization in argon at 1000 °C for 6 h. The carbonized wood piece was then diced into small sections of 1 × 0.5 cm. Hydrolyzable chestnut tannins were dissolved in 0.1 M $HClO_4$ at a concentration of 10 g L^{-1} and the same amount of pyrrole was added to the mixture. The solution was stirred using a magnetic stir bar until a homogeneous appearance of the two miscible constituents was achieved. To electropolymerize the Tn/Ppy composites on Au/carbonized wood substrate, a galvanostatic polarization technique with a current density of 0.25 mA cm^{-2} was applied in a typical three electrode setup with the Au/carbonized wood electrode as working electrode, Pt foil counter electrode, and Ag/AgCl reference electrode in tannins and pyrrole solution. Electropolymerization is greatly beneficial because by simply adjusting the time and applied current certain properties of the polymerized film may be easily controlled, such as its mass, thickness, and morphology. As the morphology of the synthesized film was very uniform with microspheroidal grains, as observed in the SEM, low current density (0.25 mA cm^{-2}) was applied for all the experiments. This behavior is perhaps due to the short chain length of the Ppy network, because of some side reaction, which leads to the formation of defects along the chain and further reduction the conductivity of the entire electrode. On the basis of these observations, the electropolymerization time was adjusted to 5 min to get an optimized specific capacitance at a certain concentration (10 g L^{-1}). For the carbonized wood electrode, 30 min deposition time was used to obtain a significant high mass loading. The electrodes were rinsed thoroughly with DI water after deposition and dried under vacuum for at least 8 h at room temperature.

Gel Permeation Chromatography (GPC) Analysis. Tannins (20 mg) were acetylated in a mixture of pyridine (0.5 mL) and acetic anhydride (0.5 mL) at 40 °C while stirring. After 24 h, the reaction was quenched by addition of methanol (0.2 mL). The acetylation reagents were then removed from the reaction mixture using a stream of nitrogen gas. The sample was further dried in a vacuum oven at 40 °C overnight. The dried acetylated sample was dissolved in tetrahydrofuran (THF, Baker HPLC grade) and then filtered through a 0.45 μm polytetrafluoroethylene (PTFE) syringe filter before GPC analysis. GPC analysis was performed using an Agilent 1050 HPLC with three GPC columns connected in series (Polymer Laboratories, 300 × 7.5 mm) packed with polystyrene–divinylbenzene copolymer gel (10 μm diameter beads) having nominal pore diameters of 10^4, 10^3, and 50 Å. The THF eluent was operated at a flow rate of 1 mL/min and 25 μL injection volume were used. The GPC was attached to a diode array detector measuring absorbance at 260 ± 40 nm. Using polystyrene standards, retention time was converted into estimated molecular weight (MW) by applying a calibration curve (Polymer Laboratories, MW = 580 to 2,200,000 Da) with toluene (MW = 92 Da). The molecular weight of the tannin sample was estimated from the elution volume corresponding to the maximum OD of the injected sample and given as peak average MW (MWp or Mp).

Quantitative ^{13}C Nuclear Magnetic Resonance. NMR spectrum of acetylated tannin sample was acquired at 25 °C on a Bruker 400 MHz NMR spectrometer with a 5 mm BBO probe with a Z gradient at 40 °C. One hundred milligrams of the tannin sample was acetylated under the same conditions mentioned above and then dissolved in 0.6 mL of DMSO-d_6. For the quantitative ^{13}C NMR, the inverse-gated decoupling sequence was used with a pulse program of ZGIG. Spectrum was recorded with a sweep width of 350 ppm. A total of 20 000 scans were performed. An acquisition time of 0.94 s was used. A relaxation delay was 10 s. Tetramethylsilane was used as an internal reference. Chromium(III) acetylacetonate (0.8 mg) was added to the tannin solution to provide complete relaxation of all nuclei. Benzaldehyde was used as an internal standard to quantify phenolic hydroxyl content in the tannin sample.

Solid-State NMR. High-resolution ^{13}C CP/MAS NMR measurements were performed using a Bruker Avance 200 MHz spectrometer operating at 50.13 MHz at room temperature. The spinning speed was 6000 Hz, acquisition time 48.3 ms, and the delay between pulses of two second.

Optical Characteristics Measurements by Ultraviolet–Visible (UV–vis) Spectroscopy and Confocal Microscopy. A solution of hydrolyzable chestnut tannins at a concentration of 10 g L^{-1} in DI water was initially prepared and then subjected to a 100 fold dilution. A 2 mL aliquot was taken from this dilution and characterized with an Agilent 8453 UV–vis spectrometer (10 mm path length quartz cuvette) at 1 nm intervals over the wavelength ranging from 200 to 1000 nm. To further illustrate the optical properties of tannins, preparation was dropped onto transverse and longitudinal cross sections of the carbonized wood substrate and then viewed by Olympus FV1000 multiphoton confocal microscope. This microscope was operated in the fluorescence mode with a 1.32-numerical aperture, using argon ion laser excitation at 405 and 488 nm and emission <530 nm. Scanning over a smaller field size allowed higher-magnification images to be taken.

Characterization of the Composites Electrode. The conductivity of the Tn/Ppy composites was measured by a four-point probe instrument using a freestanding sample produced on indium tin oxide electrode and separated by sonicating in DI water. To acquire the thickness relation to the deposition time, thickness profiles were measured with a mechanical profilometer (Dektak 6M). High-angle SEM images were also used to confirm the thickness variation along with the deposition time further. To characterize the morphologies and architecture of the Tn/Ppy deposited on carbonized wood electrode, two samples were freeze-fractured, while immersed in liquid nitrogen in transverse and longitudinal directions separately. The cross section cuts of the Tn/Ppy composites on carbonized wood electrode were scanned by a field emission

DOI: 10.1021/acs.nanolett.7b04242
Nano Lett. XXXX, XXX, XXX–XXX

scanning electron microscope [Supra 25] using an accelerating voltage of 5KeV. The high angle images were taken by tilting the stage at 80° and the thickness was corrected for the tilt. It is worth mentioning that there were no contrast differences between tannins and Ppy, due to the high molecular miscibility, to distinctly identify them within the composites material.

Electrochemical Analysis. The electrochemical characterization was carried out in a standard three electrode setup with a platinum foil counter electrode, Ag/AgCl reference electrode, and 0.1 M $HClO_4$ aqueous electrolyte, using a Biologic Electrochemical Station SP150 at room temperature. The cyclic voltammetry was accomplished at several scan rates ranging from 2 mV to 100 mV/s for Au substrate and 10 to 200 mV/s for carbonized wood substrate. The charge−discharge curves were performed within a voltage window of 0.1 to 0.7 V, and the electrochemical impedance spectroscopy was conducted at a frequency range of 100 kHz to 0.01 Hz at the open circuit potential with 10 mV amplitude.

■ ASSOCIATED CONTENT

Supporting Information

The Supporting Information is available free of charge on the ACS Publications website at DOI: 10.1021/acs.nanolett.7b04242.

Additional information and figures (PDF)

■ AUTHOR INFORMATION

Corresponding Author

*E-mail: h.zhu@neu.edu.

ORCID

Peter N. Ciesielski: 0000-0003-3360-9210

Hongli Zhu: 0000-0003-1733-4333

Notes

The authors declare no competing financial interest.

■ ACKNOWLEDGMENTS

This research was financially supported by the start-up grant and Tier1 fund to H.Z. from Northeastern University. Funding for R.K., P.N.C., and M.E.H. was provided by the NREL Laboratory Directed Research and Development (LDRD) program. We would like to thank Lei Yang for carbonizing the wood pieces for the preparation of the CW substrate. We also appreciate the use of the facilities at George J. Kostas Nanoscale Technology and Manufacturing Research Center at Northeastern.

■ REFERENCES

(1) Leguizamon, S.; Díaz-Orellana, K. P.; Velez, J.; Thies, M. C.; Roberts, M. E. *J. Mater. Chem. A* **2015**, *3*, 11330−11339.

(2) Zhang, L.; Liu, Z.; Cui, G.; Chen, L. *Prog. Polym. Sci.* **2015**, *43*, 136−164.

(3) Cottineau, T.; Toupin, M.; Delahaye, T.; Brousse, T.; Bélanger, D. *Appl. Phys. A: Mater. Sci. Process.* **2006**, *82*, 599−606.

(4) Simon, P.; Gogotsi, Y. *Nat. Mater.* **2008**, *7*, 845−854.

(5) Navarro-Suárez, A. M.; Casado, N.; Carretero-González, J.; Mecerreyes, D.; Rojo, T. *J. Mater. Chem. A* **2017**, *5*, 7137−7143.

(6) Song, Z.; Zhou, H. *Energy Environ. Sci.* **2013**, *6*, 2280−2301.

(7) Gracia, R.; Mecerreyes, D. *Polym. Chem.* **2013**, *4*, 2206−2214.

(8) Kim, S. Y.; Jeong, H. M.; Kwon, J. H.; Ock, I. W.; Suh, W. H.; Stucky, G. D.; Kang, J. K. *Energy Environ. Sci.* **2015**, *8*, 188−194.

(9) Kumar, P.; Di Mauro, E.; Zhang, S.; Pezzella, A.; Soavi, F.; Santato, C.; Cicoira, F. *J. Mater. Chem. C* **2016**, *4*, 9516−9525.

(10) Milczarek, G.; Inganäs, O. *Science* **2012**, *335*, 1468−1471.

(11) Milczarek, G. *Electroanalysis* **2007**, *19*, 1411−1414.

(12) Geng, X.; Zhang, Y.; Jiao, L.; Yang, L.; Hamel, J.; Giummarella, N.; Henriksson, G.; Zhang, L.; Zhu, H. *ACS Sustainable Chem. Eng.* **2017**, *5*, 3553−3561.

(13) Aro, T.; Fatehi, P. *ChemSusChem* **2017**, *10*, 1861.

(14) Melone, F.; Saladino, R.; Lange, H.; Crestini, C. *J. Agric. Food Chem.* **2013**, *61*, 9307−9315.

(15) Khanbabaee, K.; van Ree, T. *Nat. Prod. Rep.* **2001**, *18*, 641−649.

(16) Arapitsas, P. *Food Chem.* **2012**, *135*, 1708−1717.

(17) Schofield, P.; Mbugua, D. M.; Pell, A. N. *Anim. Feed Sci. Technol.* **2001**, *91*, 21−40.

(18) Hathway, D. *Biochem. J.* **1958**, *70*, 34.

(19) Vázquez, G.; Fontenla, E.; Santos, J.; Freire, M. S.; González-Álvarez, J.; Antorrena, G. *Ind. Crops Prod.* **2008**, *28*, 279−285.

(20) Elgailani, I. E. H.; Ishak, C. Y. *Pak. J. Anal. Environ. Chem.*, **2016**, *17*,10.21743/pjaec/2016.06.007

(21) Liao, R.-Z.; Kärkäs, M. D.; Lee, B.-L.; Åkermark, B.; Siegbahn, P. E. M. *Inorg. Chem.* **2015**, *54*, 342−351.

(22) Chen, C.; Zhang, Y.; Li, Y.; Dai, J.; Song, J.; Yao, Y.; Gong, Y.; Kierzewski, I.; Xie, J.; Hu, L. *Energy Environ. Sci.* **2017**, *10*, 538−545.

(23) Shen, F.; Luo, W.; Dai, J.; Yao, Y.; Zhu, M.; Hitz, E.; Tang, Y.; Chen, Y.; Sprenkle, V. L.; Li, X.; et al. *Advanced Energy Materials* **2016**, *6*, 1600377.

(24) Widsten, P.; Heathcote, C.; Kandelbauer, A.; Guebitz, G.; Nyanhongo, G. S.; Prasetyo, E. N.; Kudanga, T. *Process Biochem.* **2010**, *45*, 1072−1081.

(25) Vázquez, G.; Pizzi, A.; Freire, M. S.; Santos, J.; Antorrena, G.; González-Álvarez, J. *Wood Sci. Technol.* **2013**, *47*, 523−535.

(26) Saminathan, M.; Tan, H. Y.; Sieo, C. C.; Abdullah, N.; Wong, C. M. V. L; Abdulmalek, E.; Ho, Y. W. *Molecules* **2014**, *19*, 7990−8010.

(27) Fu, C.; Loo, A. E. K.; Chia, F. P. P.; Huang, D. *J. Agric. Food Chem.* **2007**, *55*, 7689−7694.

(28) Navarrete, P.; Pizzi, A.; Pasch, H.; Rode, K.; Delmotte, L. *Ind. Crops Prod.* **2010**, *32*, 105−110.

(29) Falcão, L.; Araújo, M. E. M. *Journal of Cultural Heritage* **2013**, *14*, 499−508.

(30) Brousse, T.; Toupin, M.; Dugas, R.; Athouël, L.; Crosnier, O.; Bélanger, D. *J. Electrochem. Soc.* **2006**, *153*, A2171−A2180.

(31) Tsay, K.-C.; Zhang, L.; Zhang, J. *Electrochim. Acta* **2012**, *60*, 428−436.

(32) Kim, S. K.; Kim, Y. K.; Lee, H.; Lee, S. B.; Park, H. S. *ChemSusChem* **2014**, *7*, 1094−1101.

(33) Nishimiya, K.; Hata, T.; Imamura, Y.; Ishihara, S. *J. Wood Sci.* **1998**, *44*, 56−61.

(34) Choi, B. G.; Hong, W. H.; Jung, Y. M.; Park, H. *Chem. Commun.* **2011**, *47*, 10293−10295.

(35) Bae, C. J.; Erdonmez, C. K.; Halloran, J. W.; Chiang, Y. M. *Adv. Mater.* **2013**, *25*, 1254−1258.

DOI: 10.1021/acs.nanolett.7b04242
Nano Lett. XXXX, XXX, XXX−XXX